Electric-field-assisted migration and accumulation of hydrogen in silicon carbide

M. S. Janson, A. Hallén, M. K. Linnarsson, and B. G. Svensson
Department of Electronics, Royal Institute of Technology, P.O. Box E229, SE-164 40 Kista-Stockholm, Sweden

N. Nordell and S. Karlsson
IMC, P.O. Box E233, SE-164 40 Kista-Stockholm, Sweden

(Received 16 November 1999)

The diffusion of deuterium (^{2}H) in epitaxial 4H-SiC layers with buried highly Al-acceptor doped regions has been studied by secondary ion mass spectrometry. ^{2}H was introduced in the near surface region by the use of 20-keV implantation after which the samples were thermally annealed. As a result, an anomalous accumulation of ^{2}H in the high doped layers was observed. To explain the accumulation kinetics, a model is proposed where positively charged ^{2}H ions are driven into the high doped layer and become trapped there by the strong electric field at the edges. This effect is important for other semiconductors as well, since hydrogen is a common impurity present at high concentrations in many semiconductors.

Numerous experiments have been performed to establish the basic physical parameters connected to hydrogen diffusion in semiconductors. The dissociation energies of the various hydrogen-defect complexes can often be determined with a high accuracy[1] while it has been proven difficult to establish the intrinsic hydrogen diffusion constant.[2] For reviews see, e.g., Refs. 3 and 4. Silicon carbide (SiC) is a wide-band gap semiconductor with potential for a new generation of devices operating at high power, high frequency, and high temperature. SiC crystallizes in many different polytypes of which 4H-SiC is most favored by the device community today due to its relatively high and isotropic charge-carrier mobilities. Reports on hydrogen migration and associated complex formation in SiC are rare and only recently has it been established that hydrogen passivates the aluminum and boron acceptors in epitaxial SiC.[5] However, no quantitative data concerning the parameters of the diffusion and trapping processes have yet been published. In this study, a series of diffusion experiments has been performed where deuterium (^{2}H) was introduced into different epitaxial structures by 20-keV ion implantation. The 4H-SiC epitaxial layers were grown in a horizontal vapor-phase epitaxy reactor.[6] The samples were then annealed in a vacuum furnace so that the implanted ^{2}H, acting as a diffusion source, migrated into the epilayer. Due to the trapping of ^{2}H at implantation induced defects,[7] only a minor part of the implanted ^{2}H was free to migrate into the layer at the investigated temperatures. The chemical ^{2}H, ^{27}Al, and ^{11}B profiles were then obtained using secondary ion mass spectrometry (SIMS). In samples with a homogeneous Al and/or B acceptor doping, the ^{2}H migration followed a basic diffusion model of first-order kinetics with trapping and detrapping of ^{2}H at the acceptor atoms.[8]

However, in samples with a buried Al-doped layer of high concentration, the basic model could not explain all experimental observations of ^{2}H diffusion and accumulation: (i) The chemical content of ^{2}H in an Al layer was seen to increase as a function of anneal time at a homogeneous concentration level, i.e., with no gradient in the measured SIMS profile (Fig. 1). In the basic diffusion model, one expects a strong gradient in the [^{2}H] profile until it approaches a steady-state value at the boundary. (Brackets denote concentration values.) (ii) The accumulation rate of ^{2}H was identical in samples with different Al concentration in the buried layer, as long as the thickness of the buried layer was conserved. This contradicts first-order kinetics with trapping and detrapping, since the formation rate of ^{2}H-Al complexes is proportional to both the diffusing ^{2}H and the Al concentrations.[8] (iii) On the other hand, when comparing two samples with layers of different thicknesses but identically annealed, it was seen that the ^{2}H concentration was higher in the thinner layer although the Al concentration is ~20 times higher in the wider one. However, the thickness of the layer does not affect the ^{2}H accumulation rate in the basic model.

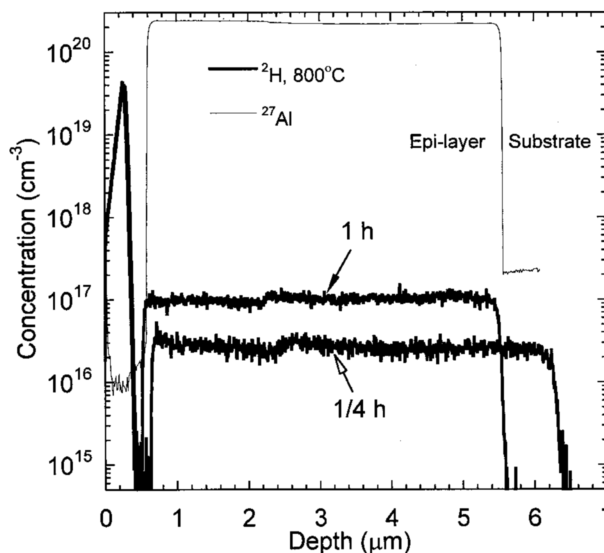

FIG. 1. SIMS measurements of ^{2}H and ^{27}Al concentrations versus depth, bold and thin lines, respectively, in a 4H-SiC Al-acceptor doped epitaxial layer with an undoped surface layer. The samples were implanted with 20-keV $^2H^+$ ions to a dose of $\sim 10^{15}$ cm^{-2} and subsequently annealed at 800 °C for $\frac{1}{4}$ and 1 h. The variation in depth of the box-shaped ^{2}H profile is attributed to variations of the epilayer thickness over the wafer surface.

 ©2000 The American Physical Society

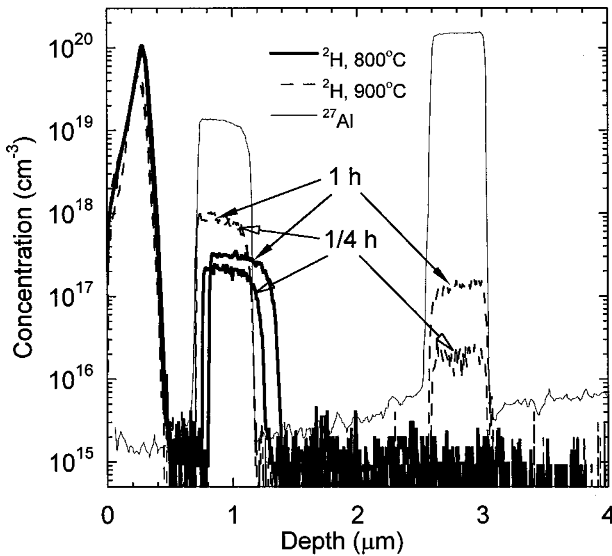

FIG. 2. SIMS measurements of ^{2}H and ^{27}Al concentrations versus depth, bold and thin lines, respectively, in a 4*H*-SiC epilayer with two highly Al doped regions surrounded by undoped epitaxial material. The samples were implanted with 20 keV $^{2}H^{+}$ ions to a dose of $\sim 10^{15}\,\mathrm{cm}^{-2}$ and subsequently annealed at 800 or 900 °C, solid and broken lines, respectively, for $\frac{1}{4}$ and 1 h.

From these observations, (i)–(iii), it is evident that a different explanation for the ^{2}H accumulation in the Al-doped epitaxial layers is needed.

Based on the assumption that ^{2}H diffuses mainly as a positively charged ion ($^{2}H^{+}$), a model is proposed to explain the unexpected behavior. The assumption that hydrogen has a positive charge state and reacts to an applied electric field has been experimentally confirmed for Si,[1,2] and recently also for SiC.[9] In those experiments the electric field was externally applied at an elevated temperature in H-passivated material. The reactivation of the dopants to a depth correlated with the maximum depth of the applied field was then measured by electrical (CV) depth profiling. The basic idea behind the proposed model is that due to the large doping gradients at the junctions between the Al layer and the surrounding low doped layers, strong built-in electric fields at the edges of the Al layer will add a drift component to the migration of $^{2}H^{+}$. The fields are directed so that the $^{2}H^{+}$ is swept into the Al layers from the surrounding low doped material. In this way the implanted ^{2}H is ''pumped'' into the Al layer at the junction closest to the surface while being retarded at the deep junction.

In order to test the validity of this model an experiment was performed with the aim to find out if the diffusing ^{2}H actually is retarded at the deep junction of the Al layer. An epitaxial layer was grown with several highly doped Al layers separated by undoped material, which for SiC means $|N_A - N_D| \leq 10^{15}\,\mathrm{cm}^{-3}$ (Fig. 2). The epilayer was then implanted by 20 keV $^{2}H^{+}$ and annealed at several temperatures and durations. Any ^{2}H migrating past the first (most shallow) Al layer would then be accumulated in the second one. However, up to 800 °C no ^{2}H was detected above the SIMS detection limit ($\sim 10^{15}\,\mathrm{cm}^{-3}$) in the second Al layer (Fig. 2). Hence, in the sample annealed at 800 °C for 1 h the concentration of ^{2}H in the second layer is at least a factor of 500 less than in the first layer, implying a very effective diffusion barrier between the layers as proposed by the model. When the anneal temperature was increased to 900 °C, [^{2}H] in the second layer reached levels above the SIMS detection limit, as depicted in Fig. 2. At 900 °C the ^{2}H concentration in the first layer is practically unchanged for the two anneal times while the concentration in the second layer increases almost by one order of magnitude between the $\frac{1}{4}$ and 1 h anneal. Another important observation is that [^{2}H] increases at a homogeneous level also in the second layer.

In addition to this experiment a detailed analysis of the diffusion and drift model is performed. To simplify the calculations the following assumptions are made. (i) Since the ^{2}H concentration never exceeds 10% of the Al concentration the electric field is assumed to be unaffected by the ^{2}H accumulation. (ii) Complex formation between ^{2}H and Al is not taken into account. This is based on the result that the ^{2}H-Al complex has proven to dissociate at temperatures as low as 300 °C.[5] (iii) The ^{2}H is assumed to migrate in the positive charge state with a constant diffusivity independent of the doping level in the sample. (iv) The implanted ^{2}H is replaced by an infinite diffusion source at concentration $^{2}H_0$ during the entire anneal. With E representing the electric field strength the differential equation including diffusion and drift of positively charged ^{2}H is written

$$\frac{\partial[^{2}\mathrm{H}]}{\partial\tau} = -\frac{q}{k_B T}\frac{\partial([^{2}\mathrm{H}]E)}{\partial x} + \frac{\partial^2[^{2}\mathrm{H}]}{\partial x^2}, \tag{1}$$

where Einstein's relation between the diffusivity (D_H) and mobility has been used. The substitution $\tau = tD_H$ (t = anneal time) is introduced to obtain a more general form of the equation. The diffusion source is implemented by the boundary condition $[^{2}\mathrm{H}]_{x=0} = {}^{2}\mathrm{H}_0$. After a sufficiently long time, diffusion and drift will balance each other and, with $\partial[^{2}\mathrm{H}]/\partial\tau|_{\tau\to\infty} = 0$ in Eq. (1), the steady-state solution is given by

$$[^{2}\mathrm{H}]|_x = {}^{2}\mathrm{H}_0 \exp\left[\frac{q}{k_B T}\int_0^x E(x')dx'\right]. \tag{2}$$

The electric-field distribution is calculated from the doping profiles using the device simulation program MEDICI with parameters according to Ref. 10. Assuming that all Al atoms in the highly doped layers are electrically active as shallow acceptors,[11] the doping concentrations in the Al layers are set to the chemical concentrations provided by SIMS. A major problem in determining the field is that the background doping between the Al layers is not accurately known. The detection limit for boron and aluminum is $\sim 1\times 10^{14}\,\mathrm{cm}^{-3}$ in the SIMS instrument, but the corresponding limit for nitrogen (N) is in the high $10^{15}\,\mathrm{cm}^{-3}$ range. Figure 3 shows the doping profile and the electrical field as calculated by MEDICI for the case of a p-type background doping ([Al] $= 5\times 10^{15}\,\mathrm{cm}^{-3}$) at 900 °C. The electrical field has a maximum value of 6.2×10^{4} V/cm and is localized at the junctions between the highly doped Al layers and the background. The electric-field distribution did not change significantly when comparing simulations at 800 and 900 °C.

Using the electric field calculated with p-type background doping (Fig. 3), Eq. (1) is solved numerically at 900 °C for $\tau = 1,2,4,\ldots,16384\times 10^{-9}\,\mathrm{cm}^{2}$. The result is displayed in Fig.

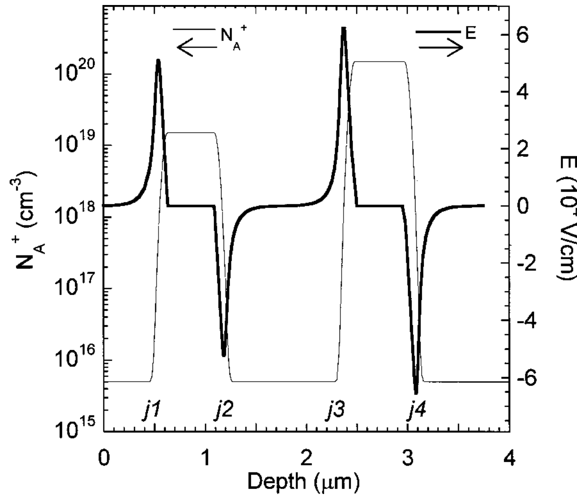

FIG. 3. The built-in electric-field distribution (bold line) as calculated by the device simulation program MEDICI for a multiple Al-layer structure with an Al background doping of $5\times10^{15}\,\mathrm{cm}^{-3}$ (thin line).

4 together with the steady-state solution given by Eq. (2) and it is clearly seen that the electric field is large enough to account for an accumulation of ^{2}H in the Al layers. When the [^{2}H] in the first layer is 50% above the surface concentration $^2\mathrm{H}_0$ (at $\tau\approx8\times10^{-9}\,\mathrm{cm}^2$) the concentration profile in the layer is almost horizontal. The ^{2}H concentration in the layer increases thereafter linearly with time until $\tau\approx256\times10^{-9}\,\mathrm{cm}^2$ after which it converges to the analytically calculated steady-state value. [^{2}H] in the second layer also builds up with a horizontal profile, delayed relative to the first layer, but the concentration increases approximately quadratic as a function of time.

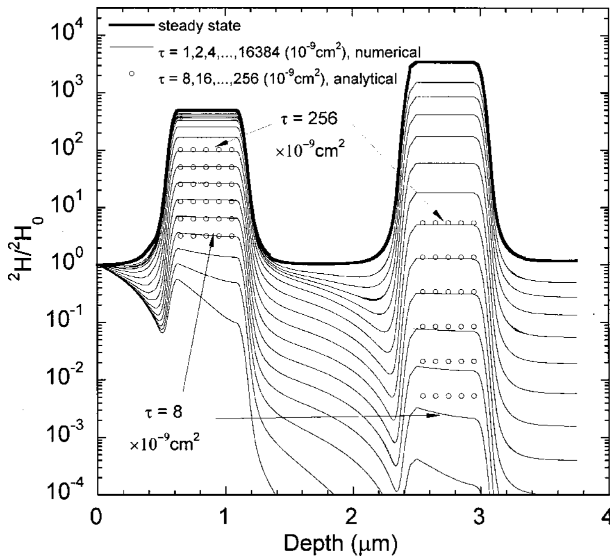

FIG. 4. Simulated diffusion of positively charged ^{2}H from an infinite source at the surface of concentration H_0 in the presence of the built-in electric field shown in Fig. 3. Equation (1) is calculated numerically for $\tau=D_H\ t=1,2,4,\ldots,\ 16384\times10^{-9}\,\mathrm{cm}^2$ (thin lines). The steady-state profile given by Eq. (2) is shown by the bold solid line. The ^{2}H concentrations in the first and second Al layers given by the analytical expressions Eqs. (3) and (4), respectively, are shown as circles for $\tau=8,16,\ldots,\ 256\times10^{-9}\,\mathrm{cm}^2$.

The linear and quadratic time dependencies of the ^{2}H accumulation in the first and second layers, respectively, can be understood by considering the following simplified model. First, the shallow junction of the first Al layer ($j1$ in Fig. 3) is assumed to act as a perfect sink for the ^{2}H diffusing between the surface and $j1$. The flux between the surface and the layer, and hence into the layer, will then be constant: $J_1=-D_H(0-{}^2\mathrm{H}_0)/x_{j1}$, where x_{jl} is the position of $j1$. If the flux out of the layer at the deep junction ($j2$ in Fig. 3) is further assumed to be negligible, the concentration in the first Al layer, $[^2\mathrm{H}]_{\mathrm{Al1}}$, is given by integrating J_l over time and dividing by the thickness of the first Al layer, Δx_{Al1}:

$$[^2\mathrm{H}]_{\mathrm{Al1}}=\frac{^2\mathrm{H}_0 D_H}{x_{j1}\Delta x_{\mathrm{Al1}}}, \tag{3}$$

which increases linearly with time. The ^{2}H concentration in the second layer, $[^2\mathrm{H}]_{\mathrm{Al1}}$, is calculated in a similar way but the corresponding ''surface'' concentration, $[^2\mathrm{H}]_{xj2+}$, (i.e., the concentration to the right of $j2$ in the low doped region) is not constant but increases as a function of time. If the ratio of the ^{2}H concentrations on each side of $j2$ is approximated by the steady-state value [Eq. (2)], then $[^2\mathrm{H}]_{xj2+}$ is proportional to $[^2\mathrm{H}]_{\mathrm{Al1}}$ at all times and the proportionality factor, k, is given by Eq. (2). Assuming that the flux between the first and second layer is quasistatic, the flux into the second layer is given by: $J_2=-D_H(0-k[^2\mathrm{H}]_{\mathrm{Al1}})/(x_{j3}-x_{j2})$, where $x_{j2,3}$ are the positions of junctions $j2$ and $j3$. $[^2\mathrm{H}]_{\mathrm{Al2}}$ is then given by integrating the time dependent flux J_2 and dividing by the thickness of the second layer, Δx_{Al2}:

$$[^2\mathrm{H}]_{\mathrm{Al2}}=\frac{^2\mathrm{H}_0 D_H^2}{2x_{j1}(x_{j3}-x_{j2})\Delta x_{\mathrm{Al1}}\Delta x_{\mathrm{Al2}}}\times\exp\left[\frac{q}{k_BT}\int_{xj2-}^{xj2+}E(x')dx'\right]t^2, \tag{4}$$

which has a quadratic time dependence. The exponential in Eq. (4) yields the proportionality factor k and the limits of the integral $xj2\pm$ are taken on each side of $j2$ where the field is close to zero. The result of the analytical expressions (3) and (4) for $\tau=8,16,\ldots,256\times10^{-9}\,\mathrm{cm}^2$ are plotted in Fig. 4 as circles and display good agreement with the numerical calculations. This means that in the case of a p-type background doping, the electric field only determines the boundary conditions between the different regions, while the rate of the ^{2}H accumulation is solely determined by unperturbed diffusion between the layers and the surface.

Simulations have also been performed based on a electric field calculated for a n-type background doping ($[N]=5\times10^{15}\,\mathrm{cm}^{-3}$) between the Al-layers. Furthermore, to investigate how complex formation affects the accumulation kinetics, trapping and de-trapping of ^{2}H by the Al atoms have also been included in the diffusion and drift model (not shown). Both these cases exhibit the same qualitative behavior as the simulations shown in Fig. 4, but with considerably higher ^{2}H steady state concentrations in the Al layers. Another quantitative difference is that the delay of the ^{2}H accumulation in the second peak relative to the first one is much greater in these simulations compared to the ones in Fig. 4.

The presented diffusion and drift model thus gives an explanation to the unexpected observations of the measured ^{2}H-profiles: the accumulation in the Al-layers with horizontal profiles, the large difference of the [^{2}H] in the first and second Al-layers as well as the dependence of the width of the Al-layer on the ^{2}H-accumulation. In the light of the new model, the experimental data suggests that the steady state level between diffusion and drift is reached in the first layer at a concentration of $\sim 1\times 10^{18}\,\mathrm{cm}^{-3}$. Furthermore, the slower than quadratic but faster than linear time dependence of the ^{2}H concentration in the second Al layer at 900 °C is consistent with the model since the quadratic time dependence of the second layer is only expected in the phase where the ^{2}H in the first layer increases linearly with time. It is, however, not possible to find a pair of simulated curves that give a good match to the measured 900 °C profiles. The best fit is obtained with the $\tau = 512$ and $2048\times 10^{-9}\,\mathrm{cm}^2$ curves which implies a diffusion constant $D_H = 6 \times 10^{-10}\,\mathrm{cm}^2/\mathrm{s}$. This value should be viewed as a lower limit since a lower p-type or a n-type background doping in the simulation would give a significantly higher value.

In summary, a model is presented to explain some unexpected results in a series of ^{2}H diffusion experiments performed using low doped epitaxial SiC layers with buried highly p-doped regions. The model involves drift of positively charged ^{2}H ions in the presence of the built-in electric fields at the junctions between low and high doped material. An experiment using a multilayer structure supports the model and the results are qualitatively reproduced by numerical simulations. Calculations show that the multilayer structure could be a useful tool to determine diffusion constants of charged species migrating at concentration levels too low for conventional techniques. The next step in this work is to repeat the experiment using samples with a well defined background doping in order to further establish the validity of the model and to determine the hydrogen diffusion constant in SiC.

The authors are grateful to Erik Danielsson for assistance with the MEDICI simulations. This work was funded by the Swedish Foundation for Strategic Research, within the SiCEP program.

[1] T. Zundel and J. Weber, Phys. Rev. B **39**, 13 549 (1989).

[2] C. H. Seager, R. A. Anderson, and D. K. Brice, J. Appl. Phys. **68**, 3268 (1990).

[3] J. I. Pankov and N. M. Johnson, *Hydrogen in Semiconductors* (Academic, New York, 1991).

[4] S. J. Pearton, *Hydrogen in Crystalline Semiconductors* (Springer-Verlag, New York, 1991).

[5] N. Achtziger, J. Grillenberger, W. Witthuhn, M. K. Linnarsson, M. Janson, and B. G. Svensson, Appl. Phys. Lett. **73**, 945 (1998).

[6] N. Nordell, A. Schöner, and S. G. Andersson, J. Electrochem. Soc. **143**, 2910 (1996).

[7] M. K. Linnarsson, J. P. Doyle, and B. G. Svensson, in *III-Nitride, SiC, and Diamond Materials for Electronic Devices*, edited by D. K. Gaskill, C. Brandt, and R. J. Nemanich, MRS Symposia Proceedings No. 423 (Materials Research Society, Pittsburgh, 1996), p. 625.

[8] M. K. Linnarsson, M. Janson, S. Karlsson, A. Schöner, N. Nordell, and B. G. Svensson, Mater. Sci. Eng., B **61-62**, 275 (1999).

[9] N. Achtziger, C. Hültsen, W. Witthuhn, M. K. Linnarsson, M. Janson, and B. G. Svensson, Phys. Status Solidi B **210**, 395 (1998).

[10] M. Bakowski, M. Gustafsson, and U. Lindefelt, Phys. Status Solidi A **162**, 421 (1997).

[11] N. Nordell, S. Savage, and A. Schöner, in *Silicon Carbide and Related Materials*, *Proceedings of International Conference on Silicon Carbide and Related Materials*, edited by S. Nakashima, H. Matsunami, S. Yoshida, and H. Harima, IOP Conf. Proc. No. 142 (Institute of Physics and Physical Society, Kyoto, 1995), pp. 573–576.